Published in *International Journal of Solids and Structures*, 2015, Vol. 63, pp. 226- 239.
doi:10.1016/j.ijsolstr.2015.03.002

A contact problem in couple stress thermoelasticity: The indentation by a hot flat punch

Th. Zisis, P.A. Gourgiotis and F. Dal Corso

Department of Civil, Environmental and Mechanical Engineering, University of Trento, Trento, I–38123, Italy

Abstract

It is well known, that thermo-elastic effects may have significant results upon the macroscopic response in the mechanics of contact. On the other hand, as the scales in the contact system reduce progressively (micro to nano–scales), the internal material lengths become important and their effect upon the macroscopic response cannot be ignored. The present work extends the classical contact solution for a hot flat punch indenting a homogeneous elastic half–plane, where heat conduction is permitted (Comninou et al., 1981), to the analogous case of an indented microstructured solid. The behavior of the indented material is modelled through the couple–stress elasticity theory, which introduces characteristic material lengths and is appropriately modified in order to incorporate the thermal effects. The problem formulation is based on singular integral equations, resulted from a treatment of the mixed boundary value problems via integral transforms and generalized functions. The results show significant departure from the predictions of classical thermoelasticity showing that the microstructural characteristics of the material should not be ignored.

Keywords: Perfect contact, Separation, Microstructure, Micromechanics, Singular integral equations, Thermal effects.

* Corresponding author. Tel.: +39 0461 282594; fax: +39 0461 282599.

E-mail address: zisis@mail.ntua.gr (Th. Zisis)

Published in *International Journal of Solids and Structures*, 2015, Vol. 63, pp. 226- 239.
doi:10.1016/j.ijsolstr.2015.03.002

1. Introduction

The contact of two bodies maintained at different temperatures yields to thermo-elastic deformations at the contact region that, although small, can affect the contact pressure distribution and, depending on the temperature difference between the two bodies, even the contact area. Assuming that the heat flows only through the contact area and that no heat flows across the exposed surfaces, theoretical investigations by Barber (1971, 1973 and 1978) on indentation problems predict that the regions near the contact area expand when the indentor's temperature is raised over a specific limit, causing the separation of the two solids, if the compressive load is maintained constant. This separation is expected to cause a reduction in the extent of the contact area between the indentor and the indented elastic body. This behavior was also experimentally confirmed by Clausing (1966) who, almost ten years earlier, had shown that the thermal contact resistance between two contacting bodies varies with the transmitted heat flux as a result of the thermo-elastically driven changes in the extend of the contact area.

It is well-known that material microstructure influences the macroscopical behavior of complex materials, such as composites, cellular materials and ceramics. In fact Maranganti and Sharma (2007) showed that gradient effects play significant role in complex materials with course-grain microstructure, while Chen et al. (1998) developed a continuum model for cellular materials and concluded that the continuum description of this class of materials obeys a gradient elasticity theory of the couple-stress type by naturally identifying the cell size with the material length scale. Size effects have been also predicted for two dimensional grid-works (Askar and Cakmak, 1968) and three dimensional cubic lattices (Lakes, 1986) and, associated with Cosserat elasticity, lead to an increase in moduli with decreasing specimen size relative to the cell size (Onck et al. 2001). Finally, strain gradient effects, even though difficult to be measured, have been observed in rigid polyurethane and polymethactylimide foams (Lakes, 1986; Anderson and Lakes, 1994).

While classical continuum theories do not incorporate internal length-scales and therefore cannot take into account micromechanical effects, the use of generalized continuum theories (see e.g. Maugin, 2010) allows to achieve a more effective description of the mechanical response when, for instance, stress concentrations appear (Georgiadis, 2003; Gourgiotis and Piccolroaz, 2014) or instability phenomena are involved (Dal Corso and Willis, 2011; Bacigalupo and Gambarotta, 2013). The need for such generalized continuum models has also been verified through experimental (Lakes

Published in *International Journal of Solids and Structures*, 2015, Vol. 63, pp. 226- 239.
doi:10.1016/j.ijsolstr.2015.03.002

et al., 1985; Beveridge et al., 2013) and theoretical (Smishlayev and Fleck, 1995; Bigoni and Drugan, 2007; Bacca et al., 2013a; 2013b; Bacigalupo, 2013) approaches.

During indentation, size effects can be dominant especially when the indentation size is comparable to the material microstructure. This process has been modeled employing classical theories by directly incorporating the microstructural characteristics into the model through purely geometrical considerations (see e.g. Chen et al., 2004; Stupkiewicz, 2007; Fleck and Zisis, 2010; Zisis and Fleck, 2010) and phenomenological approaches based on gradient elasticity / plasticity ideas, or on discrete dislocation concepts (Muki and Sternberg, 1965; Poole et al., 1996; Begley and Hutchinson, 1998; Nix and Gao, 1998; Shu and Fleck, 1998; Wei and Hutchinson, 2003; Danas et al., 2012; Zisis et al., 2014;). Even though, purely elastic indentation of materials is hard to achieve in practice (Larsson et al., 1996), elasticity can be of interest in particular cases. In fact, there are materials, such as polymers, that exhibit significant size effects also in the elastic regime (Han and Nikolov, 2007, Nikolov et al., 2007).

In the present study, the steady-state plane-strain contact problem of the hot frictionless flat punch indenting a couple-stress elastic half-plane is investigated for the first time to analyze the influence of the internal length scale upon the macroscopic response. In addition to the dependence of the response upon the heat flux amount from the indentor to the substrate and the magnitude of the indentation load observed in the classical framework, it is shown that the type of contact (perfect contact throughout the width of the indentor or separation near the corners of the punch) occurring is strongly affected by the microstructural characteristics of the material. The opposite problem of a cool flat punch indenting an elastic half-plane with microstructure, characterized by the possibility of having imperfect contact (Barber, 1971; 1973; 1978 and Comninou and Dundurs, 1979), will be a subject of a future work.

The paper is organized as follows. In Sections 2 and 3 the fundamental equations of couple–stress thermoelasticity are summarized and particularized to plane–strain case. In Section 4 the problem of the indentation of an elastic half–plane by a hot flat punch is formulated and the appropriate boundary conditions are described. The mixed boundary value problem is attacked via Fourier transforms and singular integral equations (Sections 5 and 6). Accordingly, the integral equations are solved by employing analytical and numerical considerations in Section 7. The results are discussed in detail in the final part.

Published in *International Journal of Solids and Structures*, 2015, Vol. 63, pp. 226- 239.
doi:10.1016/j.ijsolstr.2015.03.002

The attained results have genuine practical application in qualitatively identifying the influence of length scale effects in solids, a requirement of practical importance for the advanced design of materials and structures.

2. Fundamentals of couple-stress thermoelasticity

One of the most effective generalized continuum theories is that of couple–stress elasticity, also known as Cosserat theory with constrained rotations (Mindlin and Tiersten, 1962; Koiter, 1964). In this theory, the modified strain–energy density and the resulting constitutive relations involve, besides the usual infinitesimal strains, certain strain gradients known as the rotation gradients. The generalized stress–strain relations for the isotropic case include, in addition to the conventional pair of elastic constants, two new elastic constants, one of which is expressible in terms of a material parameter ℓ that has dimension of [length]. The presence of this length parameter, in turn, implies that the modified theory encompasses the possibility of size effects. This theory was extended by Nowacki (1966) who derived constitutive equations on the basis of thermodynamics of irreversible processes and provided the fundamental differential equations of couple-stress thermoelasticity.

We begin by giving an account of the theory of couple–stress thermoelasticity as introduced by Nowacki (1966). In the absence of inertia effects, the balance laws for the linear and angular momentum lead to the following force and moment equations of equilibrium (Mindlin and Tiersten, 1962)

$$\sigma_{ji,j} + X_i = 0 \quad , \tag{1}$$

$$e_{ijk}\sigma_{jk} + \mu_{ji,j} + Y_i = 0 \quad , \tag{2}$$

where a Cartesian rectangular coordinate system *Oxyz* is used along with indicial notation and summation convention. In these equations σ_{ij} is the force–stress tensor, μ_{ij} is the couple-stress tensor, X_i denotes components of the body-force vector referred to a body unit, and Y_i denotes the components of the body–couple vector, a comma denotes partial differentiation and e_{ijk} is Levi–Civita alternating symbol. Further, σ_{ij} can be decomposed into its symmetric and anti-symmetric components as follows

Published in *International Journal of Solids and Structures*, 2015, Vol. 63, pp. 226- 239.
doi:10.1016/j.ijsolstr.2015.03.002

$$\sigma_{ij} = \tau_{ij} + \alpha_{ij} \quad , \tag{3}$$

with $\tau_{ij} = \tau_{ji}$ and $\alpha_{ij} = -\alpha_{ji}$, whereas it is advantageous to decompose μ_{ij} into its deviatoric $\mu_{ij}^{(D)}$ and spherical $\mu_{ij}^{(S)}$ parts in the following manner

$$\mu_{ij} = m_{ij} + \frac{1}{3}\delta_{ij}\mu_{kk} \quad , \tag{4}$$

with $\mu_{ij}^{(D)} = m_{ij}$, $\mu_{ij}^{(S)} = (1/3)\delta_{ij}\mu_{kk}$, and δ_{ij} is the Kronecker delta. Now, with the help of the Green-Gauss theorem and employing the moment equation of equilibrium (2), one may obtain the anti-symmetric part of the stress tensor as

$$\alpha_{ij} = -\frac{1}{2}e_{ijk}\left(\mu_{pk,p} + Y_k\right) . \tag{5}$$

from which follows that the stress tensor is symmetric in the absence of body couples and for a vanishing divergence of couple-stresses. Finally, combining (1)-(5) yields the final equation of equilibrium which involves only the symmetric part stress tensor and the deviatoric part of the couple-stress tensor

$$\tau_{ji,j} - \frac{1}{2}e_{jki}\left(m_{pj,pk} + Y_{j,k}\right) + X_i = 0 . \tag{6}$$

Concerning the kinematical description of the continuum, the following primary kinematical fields are defined in the framework of the geometrically linear theory

$$\varepsilon_{ij} = \frac{1}{2}\left(u_{j,i} + u_{i,j}\right) \quad , \qquad \omega_i = \frac{1}{2}e_{ijk}u_{k,j} \quad , \qquad \kappa_{ij} = \omega_{j,i} \quad , \tag{7}$$

Published in *International Journal of Solids and Structures*, 2015, Vol. 63, pp. 226- 239.
doi:10.1016/j.ijsolstr.2015.03.002

where ε_{ij} is the strain tensor, ω_i is the rotation vector, and κ_{ij} is the curvature tensor (i.e. the gradient of rotation or the curl of the strain) expressed in dimensions of [length]$^{-1}$, which by definition is traceless: $\kappa_{ii}=0$ since $\omega_{i,i}=0$. Accordingly, the compatibility equations for the kinematical fields in (7) are (Naghdi, 1965)

$$e_{ipm}e_{mjk}\varepsilon_{ij,k}+e_{pjm}\kappa_{mj}=0\ , \quad e_{ikm}e_{jpm}\kappa_{ij,k}=0\ . \tag{8}$$

where the elimination of κ_{ij} between (8) leads to the usual Saint Venant's compatibility equations for the strain tensor components.

Regarding the boundary conditions, we note that in the constrained couple-stress theory the normal component of the rotation vector is fully specified by the distribution of tangential displacements over the boundary. This implies that the traction boundary conditions, at any point on a *smooth* boundary or section, consist of the following three *reduced* force-tractions and two *tangential* couple-tractions (Mindlin and Tiersten, 1962; Koiter, 1964)

$$P_i^{(n)}=\sigma_{ji}n_j-\frac{1}{2}e_{ijk}n_j m_{(nn),k}\ , \tag{9}$$

$$R_i^{(n)}=m_{ji}n_j-m_{(nn)}n_i\ , \tag{10}$$

where $m_{(nn)}=n_i n_j m_{ij}$ is the normal component of the deviatoric couple-stress tensor m_{ij}, and n_i are the components of the unit vector outward normal to the surface.

The principle of conservation of energy written for an arbitrary volume V of the body, bounded by a *smooth* surface A , has the form

$$\underbrace{\int_V \dot{U}dV}_{\substack{\text{rate of internal}\\ \text{energy of the volume}}} = \underbrace{\int_V \left(X_i\dot{u}_i+Y_i\dot{\omega}_i\right)dV}_{\substack{\text{rate of work of body forces}\\ \text{and body couples}}} + \underbrace{\int_A \left(P_i^{(n)}\dot{u}_i+R_i^{(n)}\dot{\omega}_i\right)dA}_{\substack{\text{rate of work of force}\\ \text{and couple tractions}}} - \underbrace{\int_A q_i n_i dA}_{\substack{\text{heat transferred by}\\ \text{heat conduction}}}\ , \tag{11}$$

Published in *International Journal of Solids and Structures*, 2015, Vol. 63, pp. 226- 239.
doi:10.1016/j.ijsolstr.2015.03.002

where U is the internal energy, q_i is the component of the heat-flux vector, and the superimposed dot denotes differentiation with respect to time. By using the divergence theorem and the definitions in (9) and (10) in conjunction with the equations of equilibrium (1) and (2), the equation of the energy conservation (11) localizes in the form

$$\dot{U} = \tau_{ij}\dot{\varepsilon}_{ij} + m_{ij}\dot{\kappa}_{ij} - q_{i,i} \ . \tag{12}$$

Further, the equation of entropy balance is written as (Green and Adkins, 1960)

$$\underbrace{\int_V \dot{S} dV}_{\substack{\text{rate of increase} \\ \text{of entropy}}} = \underbrace{-\int_A \frac{q_i n_i}{T} dA}_{\substack{\text{rate of entropy} \\ \text{supplied to the} \\ \text{volume across} \\ \text{the surface}}} + \underbrace{\int_V \Theta dV}_{\substack{\text{rate of production} \\ \text{of entropy due to} \\ \text{heat conduction}}} \tag{13}$$

where S is the entropy per unit volume, T is the temperature, and Θ represents the rate of production of entropy per unit volume of the material due to heat conduction. Using the divergence theorem and assuming that the volume is arbitrary, Eq. (13) can be written in the local form as

$$\dot{S} = \Theta - \frac{q_{i,i}}{T} + \frac{q_i T_{,i}}{T^2} \ , \tag{14}$$

so that, eliminating $q_{i,i}$ from (12) and (14), we obtain

$$\dot{U} = \tau_{ij}\dot{\varepsilon}_{ij} + m_{ij}\dot{\kappa}_{ij} + T\dot{S} - T\left(\Theta + \frac{q_i T_{,i}}{T^2}\right) \ . \tag{15}$$

Accordingly, introducing the expression for the Helmholtz free energy $W = U - TS$ and assuming that W is a function of the independent variables ε_{ij}, κ_{ij} and T, we obtain the following relations (Nowacki, 1966)

$$\tau_{ij} = \frac{\partial W}{\partial \varepsilon_{ij}} \ , \quad m_{ij} = \frac{\partial W}{\partial \kappa_{ij}} \ , \quad S = -\frac{\partial W}{\partial T} \ , \quad \Theta + \frac{q_i T_{,i}}{T^2} = 0 \ . \tag{16}$$

Published in *International Journal of Solids and Structures*, 2015, Vol. 63, pp. 226- 239.
doi:10.1016/j.ijsolstr.2015.03.002

In accordance with the thermodynamics of irreversible processes, we postulate that: $\Theta \geq 0$, which implies that: $-q_i T_{,i} / T^2 \geq 0$. The latter inequality is satisfied when the Fourier law of thermal conductivity is assumed, which for an isotropic and homogeneous body becomes

$$q_i = -k\theta_{,i}\,, \tag{17}$$

where k is the conductivity coefficient, $\theta = T - T_0$ is the temperature change measured from T_0, the absolute temperature of the solid in its reference state of uniformly zero stress and strain. Thus, in view of equation (14) and taking into account the last relation of (16) , we derive the heat conduction equation as

$$T\dot{S} = k\theta_{,ii}\ . \tag{18}$$

Assuming a linear and isotropic material response, we expand the free energy density $W\left(\varepsilon_{ij}, \kappa_{ij}, T\right)$ in the neighborhood of the natural state $W\left(\mathbf{0}, \mathbf{0}, T_0\right)$ as (Nowacki, 1966)

$$W = \frac{1}{2}\lambda\varepsilon_{ii}\varepsilon_{jj} + \mu\varepsilon_{ij}\varepsilon_{ij} + 2\eta\kappa_{ij}\kappa_{ij} + 2\eta'\kappa_{ij}\kappa_{ji} - \beta\varepsilon_{kk}\theta - \frac{m}{2}\theta^2\ , \tag{19}$$

where $\left(\lambda, \mu, \eta, \eta'\right)$ are material constants which refer to the isothermal case. The moduli $\left(\lambda, \mu\right)$ have the same meaning as the Lamè constants of classical elasticity theory and are expressed in dimensions of [force][length]$^{-2}$, whereas the moduli $\left(\eta, \eta'\right)$ account for couple–stress effects and are expressed in dimensions of [force]. In addition, $\beta = \left(3\lambda + 2\mu\right)\alpha$ with α being the coefficient of thermal expansion, $m = -\partial^2 W\left(0,0,T_0\right)/\partial T^2$, and assuming positive definiteness of the internal energy the material parameters satisfy the following inequalities (Mindlin and Tiersten, 1962)

$$3\lambda + 2\mu > 0\ ,\ \mu > 0\ ,\ \eta > 0\ ,\ -1 < \frac{\eta'}{\eta} < 1\ . \tag{20}$$

Published in *International Journal of Solids and Structures*, 2015, Vol. 63, pp. 226- 239.
doi:10.1016/j.ijsolstr.2015.03.002

Now, making use of the relations (16), we obtain the generalized Duhamel-Neumann constitutive equations for a thermo-elastic couple-stress medium

$$\tau_{ij} = \lambda \varepsilon_{kk} \delta_{ij} + 2\mu \varepsilon_{ij} - \beta \theta \delta_{ij} \ , \quad m_{ij} = 4\eta \kappa_{ij} + 4\eta' \kappa_{ji} \ , \tag{21}$$

$$S = \beta \varepsilon_{kk} + m\theta \ . \tag{22}$$

It is interesting to note that the term $\kappa_{kk}\theta$ does not appear in (19) since the curvature tensor is traceless. Therefore, in contrast with the micropolar (unconstrained Cosserat) elasticity (see e.g. Nowacki, 1986), the couple-stresses in $(21)_2$ do not depend upon the temperature, whereas the entropy in (22) does not depend upon the trace of the curvature.

Incorporating now the constitutive relations (21) into the equation of equilibrium (6) and using the geometric relations in (7), one may obtain the displacement equations of equilibrium, in the absence of body forces and body couples, as

$$\mu u_{i,jj} + (\lambda + \mu) u_{j,ji} - \mu \ell^2 \left(u_{i,jjkk} - u_{j,jikk} \right) = \beta \theta_{,i} \ , \tag{23}$$

where $\ell \equiv (\eta/\mu)^{1/2}$ is a characteristic material length. Note that the multiplication of ℓ with the higher-order term reveals the *singular-perturbation* character of the couple-stress theory and the emergence of associated *boundary-layer* effects. As $\ell \to 0$, the equations of classical linear isotropic thermoelasticity are recovered from (23)[1].

Finally, assuming that $|\theta/T_0| << 1$ and that there are no heat sources within the body, the following equation of thermal conductivity is derived (Nowacki, 1966)

[1] Experiments with phonon dispersion curves indicate that for most metals, the characteristic internal length is of the order of the lattice parameter, about 0.25nm (Zhang and Sharma, 2005a) while other small–molecule materials have larger internal characteristic lengths. For example, for the semiconductor gallium arsenide (GaAs), Zhang and Sharma (2005b) estimated a characteristic length of about 0.82nm, while Lakes (1995) estimated a microstructural length for graphite H257 of the order of 2.8nm. Furthermore, foam and cellular materials exhibit a characteristic length that is comparable to the average cell size whereas in laminates is of the order of the laminate thickness. In particular for dense polyurethane foams the microstructural length may be equal to 0.33mm while for human bones about 0.5mm (see Lakes, 1995).

Published in *International Journal of Solids and Structures*, 2015, Vol. 63, pp. 226- 239.
doi:10.1016/j.ijsolstr.2015.03.002

$$\theta_{,jj} - \frac{c_\varepsilon}{k}\dot{\theta} - \frac{\beta T_0}{k}\dot{\varepsilon}_{kk} = 0 \ , \tag{24}$$

where $c_\varepsilon = mT_0$ is the specific heat at constant deformation. Equations (23) and (24) constitute the governing set of the field equations in the linear theory of couple-stress thermoelasticity. Note that (24) has the same form as in the classical theory.

3. Basic equations in plane–strain

The governing equations presented for linear and isotropic couple-stress thermoelasticity are particularized here to the plane strain case[2]. For a body that occupies a domain in the (x, y)–plane under conditions of plane strain, the displacement field takes the general form:

$$u_x \equiv u_x(x, y) \neq 0 \,, \quad u_y \equiv u_y(x, y) \neq 0 \,, \quad u_z \equiv 0 \,. \tag{25}$$

so that, except for $\omega_z \equiv \omega$ and $(\kappa_{xz}, \kappa_{yz})$, all other components of the rotation vector and the curvature tensor vanish. The non-vanishing components of the stress and couple-stress tensors are derived from (3), (5) and (21). Vanishing body forces and body couples are assumed in what follows. In view of the above, the following kinematic relations are obtained

$$\varepsilon_{xx} = \frac{\partial u_x}{\partial x} \,, \quad \varepsilon_{yy} = \frac{\partial u_y}{\partial y} \,, \quad \varepsilon_{xy} = \varepsilon_{yx} = \frac{1}{2}\left(\frac{\partial u_y}{\partial x} + \frac{\partial u_x}{\partial y}\right) \,, \tag{26}$$

$$\omega = \frac{1}{2}\left(\frac{\partial u_y}{\partial x} - \frac{\partial u_x}{\partial y}\right), \quad \kappa_{xz} = \frac{\partial \omega}{\partial x} \,, \quad \kappa_{yz} = \frac{\partial \omega}{\partial y} \,. \tag{27}$$

Further, the stress and couple-stress equations of equilibrium (1) and (2) are

[2] An interesting exposition of the theory under plane-strain conditions was given in the work by Muki and Sternberg (1965), and more recently by Gourgiotis and Piccolroaz (2014) including also inertial and micro-inertial effects.

Published in *International Journal of Solids and Structures*, 2015, Vol. 63, pp. 226- 239.
doi:10.1016/j.ijsolstr.2015.03.002

$$\frac{\partial \sigma_{xx}}{\partial x}+\frac{\partial \sigma_{yx}}{\partial y}=0\,,\qquad \frac{\partial \sigma_{xy}}{\partial x}+\frac{\partial \sigma_{yy}}{\partial y}=0\,,\qquad \sigma_{xy}-\sigma_{yx}+\frac{\partial m_{xz}}{\partial x}+\frac{\partial m_{yz}}{\partial y}=0\,, \tag{28}$$

while the constitutive equations furnish

$$\begin{aligned}
\varepsilon_{xx} &= (2\mu)^{-1}\left[\,\sigma_{xx}-\nu\left(\sigma_{xx}+\sigma_{yy}\right)\right]+(2\mu)^{-1}(1-2\nu)\,\beta\theta\,,\\
\varepsilon_{yy} &= (2\mu)^{-1}\left[\,\sigma_{yy}-\nu\left(\sigma_{xx}+\sigma_{yy}\right)\right]+(2\mu)^{-1}(1-2\nu)\,\beta\theta\,,\\
\varepsilon_{xy} &= (4\mu)^{-1}\left(\sigma_{xy}+\sigma_{yx}\right)\,,
\end{aligned} \tag{29}$$

and

$$\kappa_{xz}=\left(4\mu\ell^{2}\right)^{-1}m_{xz}\,,\quad \kappa_{yz}=\left(4\mu\ell^{2}\right)^{-1}m_{yz}\,, \tag{30}$$

where μ, ν and ℓ, in this order, stand for the shear modulus, Poisson's ratio, and the characteristic material length of couple–stress theory (Mindlin and Tiersten, 1962).

Combing now the previous equations, we obtain the following stress and couple–stress equations of compatibility

$$\frac{\partial^{2}\sigma_{xx}}{\partial y^{2}}+\frac{\partial^{2}\sigma_{yy}}{\partial x^{2}}-\nu\nabla^{2}\left(\sigma_{xx}+\sigma_{yy}\right)-\frac{\partial^{2}}{\partial x\partial y}\left(\sigma_{xy}+\sigma_{yx}\right)+(1-2\nu)\,\beta\nabla^{2}\theta=0\,, \tag{31}$$

$$\frac{\partial m_{xz}}{\partial y}=\frac{\partial m_{yz}}{\partial x}, \tag{32}$$

$$m_{xz}=-2\ell^{2}\frac{\partial}{\partial y}\left[\sigma_{xx}-\nu\left(\sigma_{xx}+\sigma_{yy}\right)+(1-2\nu)\,\beta\theta\right]+\ell^{2}\frac{\partial}{\partial x}\left(\sigma_{xy}+\sigma_{yx}\right)\,, \tag{33}$$

$$m_{yz}=2\ell^{2}\frac{\partial}{\partial x}\left[\sigma_{yy}-\nu\left(\sigma_{xx}+\sigma_{yy}\right)+(1-2\nu)\,\beta\theta\right]-\ell^{2}\frac{\partial}{\partial y}\left(\sigma_{xy}+\sigma_{yx}\right). \tag{34}$$

from which follows that only three of the four equations of compatibility are independent. Indeed, Eqs. (32)-(34) imply (31), while Eqs. (31), (33) and (34) yield (32) (Mindlin, 1963; Muki and Sternberg, 1965).

Published in *International Journal of Solids and Structures*, 2015, Vol. 63, pp. 226- 239.
doi:10.1016/j.ijsolstr.2015.03.002

Finally, Mindlin (1963) introduced pertinent stress functions (generalizing the Airy stress function of classical elasticity) by showing that the complete solution of equilibrium Eqs. (28) admits the following representation

$$\sigma_{xx}=\frac{\partial^2\Phi}{\partial y^2}-\frac{\partial^2\Psi}{\partial x\partial y},\quad \sigma_{yy}=\frac{\partial^2\Phi}{\partial x^2}+\frac{\partial^2\Psi}{\partial x\partial y},$$
$$\sigma_{xy}=-\frac{\partial^2\Phi}{\partial x\partial y}-\frac{\partial^2\Psi}{\partial y^2},\quad \sigma_{yx}=-\frac{\partial^2\Phi}{\partial x\partial y}+\frac{\partial^2\Psi}{\partial x^2}, \tag{35}$$

and

$$m_{xz}=\frac{\partial\Psi}{\partial x},\quad m_{yz}=\frac{\partial\Psi}{\partial y}, \tag{36}$$

where $\Phi\equiv\Phi(x,y)$ and $\Psi\equiv\Psi(x,y)$ are two arbitrary but sufficiently smooth potentials. Substitution of (35) and (36) into (33) and (34) results in the following pair of differential equations, for the stress functions

$$\frac{\partial}{\partial x}\left(\Psi-\ell^2\nabla^2\Psi\right)=-2(1-\nu)\ell^2\nabla^2\left(\frac{\partial\Phi}{\partial y}\right)-2\beta\ell^2(1-2\nu)\frac{\partial\theta}{\partial y}, \tag{37}$$

$$\frac{\partial}{\partial y}\left(\Psi-\ell^2\nabla^2\Psi\right)=2(1-\nu)\ell^2\nabla^2\left(\frac{\partial\Phi}{\partial x}\right)+2\beta\ell^2(1-2\nu)\frac{\partial\theta}{\partial x}, \tag{38}$$

which then lead to the uncoupled PDEs

$$(1-\nu)\nabla^4\Phi+\beta(1-2\nu)\nabla^2\theta=0, \tag{39}$$

$$\nabla^2\Psi-\ell^2\nabla^4\Psi=0. \tag{40}$$

To these equations we also have to add the equation of heat conductivity. Assuming no internal heat sources and steady state conditions, equation (24) simplifies to

Published in *International Journal of Solids and Structures*, 2015, Vol. 63, pp. 226- 239.
doi:10.1016/j.ijsolstr.2015.03.002

$$\nabla^2\theta = 0\,. \tag{41}$$

In addition, from (26)–(29) and (35)–(36), one can obtain the following relations connecting the displacement field in terms of Mindlin's stress functions

$$\frac{\partial u_x}{\partial x} = \frac{1}{2\mu}\left(\frac{\partial^2\Phi}{\partial y^2} - \frac{\partial^2\Psi}{\partial x\partial y} - \nu\nabla^2\Phi + (1-2\nu)\beta\theta\right), \tag{42}$$

$$\frac{\partial u_y}{\partial y} = \frac{1}{2\mu}\left(\frac{\partial^2\Phi}{\partial x^2} + \frac{\partial^2\Psi}{\partial x\partial y} - \nu\nabla^2\Phi + (1-2\nu)\beta\theta\right), \tag{43}$$

$$\frac{\partial u_x}{\partial y} + \frac{\partial u_y}{\partial x} = -\frac{1}{2\mu}\left(2\frac{\partial^2\Phi}{\partial x\partial y} - \frac{\partial^2\Psi}{\partial x^2} + \frac{\partial^2\Psi}{\partial y^2}\right). \tag{44}$$

Note that as the quantities ℓ, $\partial_x\Psi$, and $\partial_y\Psi$ tend to zero, the above representation passes over into the classical Airy's representation.

3. Formulation of the contact problem and boundary conditions

In this section, the plane-strain problem of an elastic half-plane subjected to the action of a perfectly conducting rigid flat hot indentor with sharp square corners is considered (Figure 1a and b). The indentor is pressed into the surface through the application of a load *P* (with dimensions of [force][length]$^{-1}$) normal to the half-plane and a Cartesian coordinate system *Oxyz* is considered attached at the center line of the flat punch.

Further, we assume the contact interface between the punch and half-plane to be smooth and frictionless, which means that the indentor must be lubricated. The remaining part of the half-plane surface is considered to be insulated and traction-free. Heat flow between the solids is only permitted to take place by conduction through the contact region. Moreover, the flat punch is at temperature T_p while the temperature field of the half-plane is denoted by T. Remote regions of the half-plane are assumed to be at the natural temperature T_0. In the present analysis, the punch is at higher temperature than the indented half–plane, thus excluding the possibility of imperfect contact conditions (Barber, 1978). Following normal practice, the effect of elastic deformation on the heat

Published in *International Journal of Solids and Structures*, 2015, Vol. 63, pp. 226- 239.
doi:10.1016/j.ijsolstr.2015.03.002

conduction problem is ignored and the thermal boundary conditions are therefore referred to the solid in its undeformed state.

We now postulate that the surface of the half–space $y=0$, consists of general regions of perfect contact ($x \le c$), where $2c$ is the true contact width and regions of non–contact ($x > c$). In each region the appropriate mechanical and thermal boundary conditions read (see Comninou et al., 1981)

(a) Perfect contact

$$\begin{cases} \theta = \theta_p, \\ u_y = \Delta, \\ \sigma_{yy} < 0 \end{cases} \quad \text{for} \quad |x| \le c \quad \text{and} \quad y = 0\ , \tag{45}$$

(b) Non-contact

$$\begin{cases} q = 0, \\ \sigma_{yy} = 0 \end{cases} \quad \text{for} \quad |x| > c \quad \text{and} \quad y = 0, \tag{46}$$

where Δ is a constant acting as a measure of the absolute approach of the contacting bodies, $\theta_p = T_p - T_0$, and $q(x) \equiv q_y(x,0) = -k\,\partial\theta/\partial y$ is the heat flux through the interface.

In addition, we note that since no restriction is imposed on u_x and $\partial u_x/\partial y$ under the indentor, the rotation ω is arbitrary at the contact area. Thus, by enforcing the principle of virtual power (Koiter, 1964), we approximate zero shear and couple tractions under the indentor (Shu and Fleck, 1998),

$$\sigma_{yx}(x,0) = 0 \quad \text{and} \quad m_{yz}(x,0) = 0 \quad \text{for} \quad -\infty < x < \infty\ . \tag{47}$$

in accordance with the assumption of a frictionless and smooth indentor acting on a traction-free half-plane. The above boundary conditions are accompanied by the complementary integral conditions

Published in *International Journal of Solids and Structures*, 2015, Vol. 63, pp. 226- 239.
doi:10.1016/j.ijsolstr.2015.03.002

$$\int_{-c}^{c} q(x)dx = Q\,, \quad \int_{-c}^{c} p(x)dx = P\,, \tag{48}$$

where Q is the total heat flux (positive in the direction pointing to the interior of the half-plane), P is the applied (compressive) load, and $p(x) = -\sigma_{yy}(x,0)$ is the pressure below the contact area of the indentor with the following properties:

$$p(x) = 0 \;, \quad |x| > c \qquad \text{and} \qquad p(x) = p(-x) \geq 0 \;, \; |x| < c \;. \tag{49}$$

Finally, since the indented surface is an unbounded region, the above boundary conditions must be supplemented by the regularity conditions at infinite distance from the indentor

$$\sigma_{ij}(r) \to 0 \;, \; m_{ij}(r) \to 0 \;, \quad \theta(r) \to 0 \quad \text{as} \quad r = \left(x^2 + y^2\right)^{1/2} \to \infty \;. \tag{50}$$

Equations (45)-(50) describe our mixed boundary value contact problem in the context of couple-stress thermoelasticity.

Following Comninou et al. (1981), the dimensionless parameter

$$\tau = \frac{(1+\nu)\,\mu\alpha b Q}{(1-\nu)\,kP} \;, \tag{51}$$

involving all the thermal and mechanical material parameters of the classical thermo-elastic problem, can be introduced to define the occurring type of contact under plane-strain conditions. Restricting attention to the case of hot punch ($Q > 0$), within the context of classical thermoelasticity[3], we distinguish the following two cases:

- if $\tau < 1.57$ the contact is perfect and is maintained throughout the flat punch ($c = b$; Figure 1a)

[3] Note that since in the present work the positive vertical axis points towards the interior of the half-plane, we define: $\tau = -\lambda$, where λ is the respective dimensionless parameter in Comninou et al. (1981) notation.

Published in *International Journal of Solids and Structures*, 2015, Vol. 63, pp. 226- 239.
doi:10.1016/j.ijsolstr.2015.03.002

- if $\tau > 1.57$ separation at the edges is attained ($c < b$; Figure 1b).

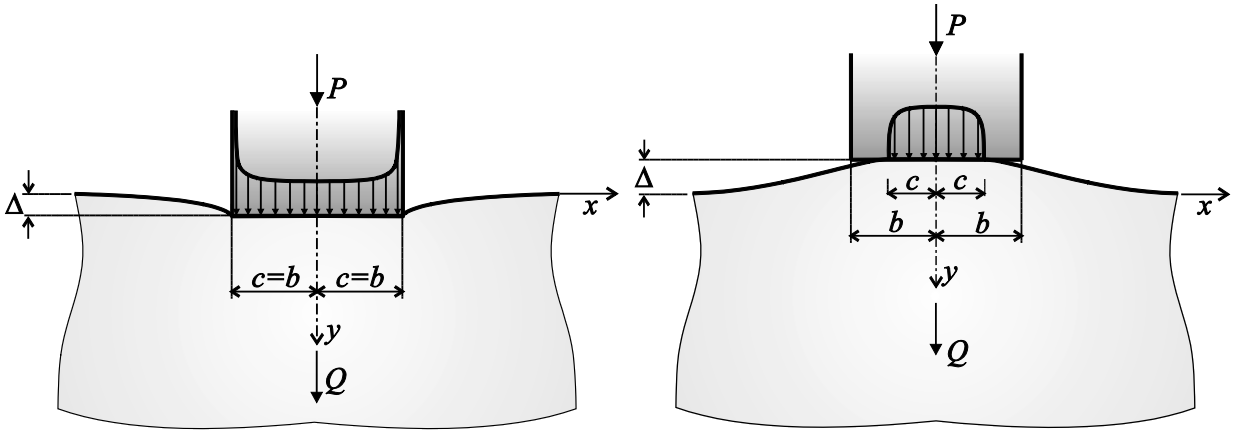

(a) (b)

Figure 1: Schematic representation of the hot punch problem, namely $Q > 0$. (a) For small possitive values of τ perfect contact will be maintained throughout the punch ($c = b$), while (b) separation ($c < b$) will occur near the edges for sufficently large possitive values of τ.

A final notice pertains to the difficulty that arises in 2D contact problems regarding the evaluation of the displacements, which is absent in the 3D cases (Johnson, 1985). Indeed, in the former case the value of the displacement of a point in a loaded elastic half–plane cannot be expressed relatively to a datum located at infinity, due to the fact that the displacements become unbounded as $O(\ln r)$, with r being the distance from the loaded zone. Thus, the normal displacement u_y can only be defined relatively to an arbitrary chosen datum. In physical terms this means that the distance Δ cannot be found by consideration of the local contact stresses alone; it is also necessary to consider the stress distribution within the bulk of each body (see also Bower, 2009).

4. Fourier transform analysis

The plane–strain contact problem is attacked with the aid of the Fourier transform on the basis of the stress function formulation summarized earlier. The direct Fourier transform and its inverse are defined as follows

Published in *International Journal of Solids and Structures*, 2015, Vol. 63, pp. 226- 239.
doi:10.1016/j.ijsolstr.2015.03.002

$$\hat{f}(\xi)=\int_{-\infty}^{\infty} f(x)e^{i\xi x}dx\ , \qquad f(x)=\frac{1}{2\pi}\int_{-\infty}^{\infty}\hat{f}(\xi)e^{-i\xi x}d\xi\ , \tag{52}$$

where $i\equiv(-1)^{1/2}$.

Transforming now the field equations (39)-(41) with $(52)_1$ provides the following ODEs for the transformed stress functions and the transformed temperature

$$\frac{d^4\hat{\Phi}}{dy^4}-2\xi^2\frac{d^2\hat{\Phi}}{dy^2}+\xi^4\hat{\Phi}=0\ , \tag{53}$$

$$\ell^2\frac{d^4\hat{\Psi}}{dy^4}-\left(1+2\ell^2\xi^2\right)\frac{d^2\hat{\Psi}}{dy^2}+\xi^2\left(1+\ell^2\xi^2\right)\hat{\Psi}=0\ , \tag{54}$$

$$\frac{d^2\hat{\theta}}{dy^2}-\xi^2\hat{\theta}=0\ . \tag{55}$$

Similarly, the following results are obtained for the Fourier transforms of the stresses, couple–stresses and displacements

$$\hat{\sigma}_{xx}=\frac{d^2\hat{\Phi}}{dy^2}+i\xi\frac{d\hat{\Psi}}{dy}\quad,\quad \hat{\sigma}_{yy}=-\xi^2\hat{\Phi}-i\xi\frac{d\hat{\Psi}}{dy}\ ,$$

$$\hat{\sigma}_{xy}=i\xi\frac{d\hat{\Phi}}{dy}-\frac{d^2\hat{\Psi}}{dy^2}\quad,\quad \hat{\sigma}_{yx}=i\xi\frac{d\hat{\Phi}}{dy}-\xi^2\hat{\Psi}\ , \tag{56}$$

$$\hat{m}_{xz}=-i\xi\,\hat{\Psi}\ ,\quad \hat{m}_{yz}=\frac{d\hat{\Psi}}{dy}\ . \tag{57}$$

$$\hat{u}_x=\frac{1}{2\mu\xi}\left(i(1-\nu)\frac{d^2\hat{\Phi}}{dy^2}-\xi\frac{d\hat{\Psi}}{dy}+i\nu\xi^2\hat{\Phi}+(1-2\nu)i\beta\hat{\theta}\right)\ ,$$

$$\hat{u}_y=\frac{1}{2\mu\xi^2}\left((1-\nu)\frac{d^3\hat{\Phi}}{dy^3}-(2-\nu)\xi^2\frac{d\hat{\Phi}}{dy}-i\xi^3\hat{\Psi}+(1-2\nu)\beta\frac{d\hat{\theta}}{dy}\right)\ . \tag{58}$$

Published in *International Journal of Solids and Structures*, 2015, Vol. 63, pp. 226- 239.
doi:10.1016/j.ijsolstr.2015.03.002

The governing equations (53)-(55) have the following general solution that is required to be bounded as $y \to +\infty$

$$\hat{\Phi}(\xi, y) = C_1(\xi) e^{-|\xi| y} + C_2(\xi) y e^{-|\xi| y} \ , \tag{59}$$

$$\hat{\Psi}(\xi, y) = C_3(\xi) e^{-|\xi| y} + C_4(\xi) e^{-\gamma y} \ , \tag{60}$$

$$\hat{\theta}(\xi, y) = C_5(\xi) e^{-|\xi| y} \ , \tag{61}$$

where $\gamma \equiv \gamma(\xi) = \left(1/\ell^2 + \xi^2\right)^{1/2}$.

Enforcing now the traction boundary conditions (47) results in the following equations for the unknown functions $C_i(\xi)$

$$C_2(\xi) = |\xi| C_1(\xi) - i\xi\left(1 - |\xi|^{-1}\gamma\right) C_4(\xi) \ , \tag{62}$$

$$C_3(\xi) = -\gamma |\xi|^{-1} C_4(\xi) \ , \tag{63}$$

where the functions $C_2(\xi)$ and $C_3(\xi)$ are related also through the compatibility equations (37) and (38) as follows

$$C_3(\xi) = -4i\ell^2 (1-\nu)\xi C_2(\xi) \ . \tag{64}$$

Further, according to $(46)_3$ and $(52)_2$, we obtain that

$$\hat{\sigma}_{yy}(\xi, 0) = \int_{-\infty}^{\infty} \sigma_{yy}(x, 0) e^{i\xi x} dx = -\int_{-c}^{c} p(x) e^{i\xi x} dx = -\hat{p}(\xi) \ , \tag{65}$$

where $\hat{p}(\xi)$ is the transformed pressure distribution below the indentor, which, taking into account $(56)_2$, can be written as

Published in *International Journal of Solids and Structures*, 2015, Vol. 63, pp. 226- 239.
doi:10.1016/j.ijsolstr.2015.03.002

$$\hat{p}(\xi)=\xi^2\hat{\Phi}+i\xi\frac{d\hat{\Psi}}{dy}\ . \tag{66}$$

Moreover, upon substituting (59) and (60) into (66) for $y=0$, and taking also into account (62)–(64), we obtain the relation

$$C_1(\xi)=\xi^{-2}\hat{p}(\xi)\ , \tag{67}$$

whereas using (61) and the definition of the heat flux, we derive

$$C_5(\xi)=k^{-1}|\xi|^{-1}\hat{q}(\xi)\ . \tag{68}$$

Finally, in view of (62)–(67), the transformed stress functions and the transformed temperature become now

$$\hat{\Phi}(\xi,y)=\left[1+\frac{|\xi|\gamma y}{\gamma-4(1-\nu)\ell^2\xi^2(|\xi|-\gamma)}\right]\frac{e^{-|\xi|y}}{\xi^2}\hat{p}(\xi)\ , \tag{69}$$

$$\hat{\Psi}(\xi,y)=-\frac{4i\ell^2(1-\nu)\left[|\xi|\gamma e^{-|\xi|y}-\xi^2e^{-\gamma y}\right]}{\left[\gamma-4(1-\nu)\ell^2\xi^2(|\xi|-\gamma)\right]\xi}\hat{p}(\xi)\ . \tag{70}$$

$$\hat{\theta}(\xi,y)=\frac{e^{-|\xi|y}}{k|\xi|}\hat{q}(\xi)\ . \tag{71}$$

5. Singular integral equation approach

Our objective now, is the determination of the contact–stress distribution $p(x)$ and the heat flux distribution $q(x)$ under the indentor and the determination of the pertinent contact length when

appropriate. For the solution of the mixed boundary value problem, we employ the method of singular integral equations. In classical elasticity, the general procedure of reducing mixed boundary value problems to singular integral equations is given, e.g., by Erdogan (1978), while various

Published in *International Journal of Solids and Structures*, 2015, Vol. 63, pp. 226- 239.
doi:10.1016/j.ijsolstr.2015.03.002

applications of this approach in classical Contact Mechanics are given in Hills et al. (1993). An example of the method within the context of couple-stress elasticity for plane-strain contact problems can be found in Zisis et al. (2014).

The definition of the inverse Fourier transform in $(52)_2$ together with Eq. $(58)_2$ lead to following equation

$$\frac{du_y}{dx}=\frac{1}{2\pi}\int_{-\infty}^{\infty}\left(\frac{-i}{2\mu\xi}\left((1-\nu)\frac{d^3\hat{\Phi}}{dy^3}-(2-\nu)\xi^2\frac{d\hat{\Phi}}{dy}-i\xi^3\hat{\Psi}\right)\right)e^{-ix\xi}d\xi$$

$$-\frac{1}{2\pi}\int_{-\infty}^{\infty}\left(\frac{i(1-2\nu)\beta}{2\mu\xi}\frac{d\hat{\theta}}{dy}\right)e^{-ix\xi}d\xi\ , \qquad (72)$$

By substituting in the above equation the expressions for the stress functions (69) and (70) at $y=0$, and taking into account (65), we obtain (Appendix)

$$\frac{du_y}{dx}=\frac{1}{2\pi}\int_{-\infty}^{\infty}\frac{i(1-\nu)|\xi|\gamma}{\mu\xi\left[4(1-\nu)\ell^2\xi^2\left(|\xi|-\gamma\right)-\gamma\right]}\cdot\left[\int_{-c}^{c}p(t)e^{i\xi t}dt\right]e^{-ix\xi}d\xi+\delta\int_0^x q(t)dt\ , \qquad (73)$$

where $\delta=(1+\nu)\alpha/k$ is the distortivity.

In view of $(45)_2$ it follows that $du_y/dx=0$ for $|x|\le c$. Thus, reversing the order of integration in (73), the problem is reduced to the following integral equation

$$\frac{1}{\mu\pi}\int_{-c}^{c}K(x-t)\,p(t)\,dt+\delta\int_0^x q(t)\,dt\ =0\ , \qquad |x|<c \qquad (74)$$

where the kernel $K(x-t)$ is defined as

$$K(x-t)=\int_0^{\infty}g(\xi)\sin\left(\xi(x-t)\right)d\xi\ , \qquad (75)$$

with

Published in *International Journal of Solids and Structures*, 2015, Vol. 63, pp. 226- 239.
doi:10.1016/j.ijsolstr.2015.03.002

$$g(\xi)=\frac{(1-\nu)\gamma}{4(1-\nu)\ell^2\xi^2(\xi-\gamma)-\gamma}\ . \tag{76}$$

In Eq. (74), passing to the limit as $\ell\to 0$ and $\delta\to 0$, one recovers the classical elasticity representation. Now, in order to make the kernel in (75) explicit and separate its singular and regular parts, it is necessary to examine the asymptotic behavior of the function $g(\xi)$ as $\xi\to\infty$. Indeed, by using theorems of the Abel–Tauber type and noting that $\lim_{\xi\to\infty} g(\xi)=g_\infty(\xi)=-\frac{1-\nu}{3-2\nu}$, we decompose $g(\xi)$ as

$$g(\xi)=g_\infty(\xi)+\left[g(\xi)-g_\infty(\xi)\right]. \tag{77}$$

Accordingly, utilizing certain results of the theory of the generalized functions and singular distributions (Roos, 1969) the kernel $K(x-t)$ becomes

$$K(x-t)=\underbrace{\int_0^\infty g_\infty(\xi)\sin\left(\xi(x-t)\right)d\xi}_{\text{singular part}}+\underbrace{\int_0^\infty\left[g(\xi)-g_\infty(\xi)\right]\sin\left(\xi(x-t)\right)d\xi}_{\text{regular part}}$$

$$=-\frac{1-\nu}{(3-2\nu)}\frac{1}{x-t}+N(x-t)\ , \tag{78}$$

where

$$N(x-t)=\int_0^\infty\left[\frac{2(1-\nu)^2\left(2\ell^2\xi^2(\gamma-\xi)-\gamma\right)}{(3-2\nu)\left(\gamma+4(1-\nu)\ell^2\xi^2(\gamma-\xi)\right)}\right]\sin\left(\xi(x-t)\right)d\xi\ , \tag{79}$$

is now a regular kernel for $x\to t$.

In view of the above, we obtain the following coupled singular integral equation relating the pressure and the heat flux under the indentor

Published in *International Journal of Solids and Structures*, 2015, Vol. 63, pp. 226- 239.
doi:10.1016/j.ijsolstr.2015.03.002

$$-\frac{(1-\nu)}{\mu\pi(3-2\nu)}\int_{-c}^{c}\frac{p(t)}{x-t}dt+\frac{1}{\mu\pi}\int_{-c}^{c}N(x-t)\,p(t)\,dt+\delta\int_{0}^{x}q(t)\,dt=0\ ,\quad |x|<c \tag{80}$$

It should be noted that the first integral in the integral equation (80) is interpreted in the Cauchy principal value sense (CPV), whereas the second integral is regular.

The integral equation for the uncoupled heat conduction problem is derived in an analogous manner. Employing the definition of the inverse Fourier transform in $(52)_2$ together with Eq. (71) leads to the following equation for the tangential derivative of the temperature at $y=0$

$$\frac{d\theta}{dx}=-\frac{1}{2\pi}\int_{-\infty}^{\infty}\frac{i\xi}{k|\xi|}\hat{q}(\xi)e^{-ix\xi}d\xi\,, \tag{81}$$

which, after reversing the order of integration and bearing in mind $(46)_1$ and $(52)_1$, can be written as

$$\frac{d\theta}{dx}=-\frac{1}{2\pi k}\int_{-c}^{c}q(t)\left[\int_{-\infty}^{\infty}i\,\mathrm{sgn}(\xi)e^{-i(x-t)\xi}d\xi\right]dt\,. \tag{82}$$

Then, since, the temperature difference is zero at the interface between the rigid indentor and the elastic half-plane (c.f. Eq.$(45)_1$) it follows that $d\theta/dx=0$ for $|x|\le c$. The heat-flux problem is then reduced to a singular integral equation of the form

$$\int_{-c}^{c}\frac{q(t)}{x-t}dt=0\ ,\quad |x|<c\ , \tag{83}$$

where the following result of the theory of generalized functions has been utilized (Roos, 1969)

$$\int_{-\infty}^{\infty}i\,\mathrm{sgn}(\xi)e^{-i(x-t)\xi}d\xi=\frac{2}{x-t}\,. \tag{84}$$

Published in *International Journal of Solids and Structures*, 2015, Vol. 63, pp. 226- 239.
doi:10.1016/j.ijsolstr.2015.03.002

The heat-conduction problem defined by (83) and the complementary condition in $(48)_1$ is not influenced by the contact stress distribution and is of standard form with solution

$$q(x)=\frac{Q}{\pi\left(c^2-x^2\right)^{1/2}}\ , \quad |x|<c\ . \tag{85}$$

Accordingly, substituting this result into equation (80) and after integration, we derive our governing singular integral equation characterizing the thermo-elastic contact problem in couple-stress elasticity

$$-\frac{1-\nu}{3-2\nu}\int_{-c}^{c}\frac{p(t)}{x-t}dt+\int_{-c}^{c}N(x-t)p(t)\,dt+\delta\mu Q\sin^{-1}\left(\frac{x}{c}\right)=0\ \ ,\ \ |x|<c\,. \tag{86}$$

The latter equation has to be supplemented with the complementary condition: $(48)_2$, for the pressure under the indentor. It is noted that Eq. (86) is uncoupled and the last term involving the heat flux plays now the role of the loading function.

The numerical solution of (86) together with the complementary condition in $(48)_2$ constitutes the aim of the remaining analysis.

6. Numerical solution

The numerical solution of the singular integral equation (86) is accomplished utilizing the appropriate collocation method. To this purpose, the following normalizations are adopted: $\tilde{x}=x/c$, $\tilde{t}=t/c$ and $\tilde{\ell}=\ell/c$. The governing singular integral equation takes then the following form

$$-\frac{1-\nu}{3-2\nu}\int_{-1}^{1}\frac{p(\tilde{t})}{\tilde{x}-\tilde{t}}d\tilde{t}+\int_{-1}^{1}\tilde{N}(\tilde{x}-\tilde{t})\,p(\tilde{t})\,d\tilde{t}+\delta\mu Q\sin^{-1}(\tilde{x})=0\quad ,\quad |\tilde{x}|<1\ , \tag{87}$$

whereas, the complementary condition in $(48)_2$ becomes

$$\int_{-1}^{1}p(\tilde{t})d\tilde{t}=Pc^{-1}, \tag{88}$$

Published in *International Journal of Solids and Structures*, 2015, Vol. 63, pp. 226- 239.
doi:10.1016/j.ijsolstr.2015.03.002

and the regular kernel $\tilde{N}\left(\tilde{x}-\tilde{t}\right)$ is defined as

$$\tilde{N}\left(\tilde{x}-\tilde{t}\right)=\int_0^{\infty}\left[\frac{2\left(1-\nu\right)^2\left(2\tilde{\ell}^2\zeta^2\left(\tilde{\gamma}-\zeta\right)-\tilde{\gamma}\right)}{\left(3-2\nu\right)\left(\tilde{\gamma}+4\left(1-\nu\right)\tilde{\ell}^2\zeta^2\left(\tilde{\gamma}-\zeta\right)\right)}\right]\sin\left(\zeta\left(\tilde{x}-\tilde{t}\right)\right)d\zeta\ , \tag{89}$$

with $\zeta=\xi c$ and $\tilde{\gamma}=\left(1/\tilde{\ell}^2+\zeta^2\right)^{1/2}$. The above convergent integral is a Fourier sine transform and can be efficiently evaluated numerically employing numerical algorithms that take into account its oscillatory character.

In what follows, we distinguish two cases, depending on the magnitude of the total heat flux and the material properties, which may occur during the thermo-elastic contact of a hot flat punch.

6.1 Perfect contact problem ($c=b$)

In this case, the contact is perfect throughout the flat punch and $c=b$ (Figure 1a). The Cauchy singular integral in Eq. (87) dominates the bounded kernel $\tilde{N}\left(\tilde{x}-\tilde{t}\right)$ and therefore determines the nature of the singularity in the pressure $p\left(\tilde{t}\right)$ at $\tilde{t}=\pm1$. Accordingly, guided by the results concerning the modification of stress singularities in the presence of couple stresses (Muki and Sternberg, 1965; Zisis et al. 2014), we introduce the appropriate unbounded fundamental solution by defining

$$p\left(\tilde{t}\right)=\sum_{n=0}^{\infty}a_nT_n\left(\tilde{t}\right)\left(1-\tilde{t}^2\right)^{-1/2}\ ,\quad \left|\tilde{t}\right|\le1\ , \tag{90}$$

where $T_n\left(\tilde{t}\right)$ are the Chebyshev polynomials of the first kind (see e.g. Abramowitz and Stegun, 1972). We note that by assuming the above pressure representation, the classical square–root stress singularity at the corners of the punch is retained also in the couple stress theory. Now, substituting (90) into the integral equation (87), one arrives at

Published in *International Journal of Solids and Structures*, 2015, Vol. 63, pp. 226- 239.
doi:10.1016/j.ijsolstr.2015.03.002

$$\sum_{n=0}^{\infty} a_n \left\{ -\frac{1-\nu}{3-2\nu} \int_{-1}^{1} \frac{T_n(\tilde{t})}{\left(1-\tilde{t}^2\right)^{1/2}\left(\tilde{x}-\tilde{t}\right)} d\tilde{t} + \int_{-1}^{1} \frac{T_n(\tilde{t})}{\left(1-\tilde{t}^2\right)^{1/2}} \tilde{N}\left(\tilde{x}-\tilde{t}\right) d\tilde{t} \right\} + \delta\,\mu Q \sin^{-1}\left(\tilde{x}\right) = 0\,, \quad \left|\tilde{x}\right| < 1 \tag{91}$$

.

Further, by employing the orthogonality properties of the Chebyshev polynomials of the first kind, the complementary condition in (88) yields: $a_0 = P\left(\pi b\right)^{-1}$, where $2b$ is the width of the flat punch. The CPV integral in (91) is evaluated by using the following properties of Chebyshev polynomials (Erdogan and Gupta, 1972)

$$\int_{-1}^{1} \frac{T_n(\tilde{t})}{\left(1-\tilde{t}^2\right)^{1/2}\left(\tilde{x}-\tilde{t}\right)} d\tilde{t} = \begin{cases} 0, & \text{if } n = 0 \\ -\pi U_{n-1}\left(\tilde{x}\right), & \text{if } n \geq 1 \end{cases}, \quad \left|\tilde{x}\right| < 1\,, \tag{92}$$

where $U_n\left(\tilde{x}\right)$ are Chebyshev polynomials of the second kind. The second integral in (91) is regular and can be readily obtained by the Gauss–Chebyshev quadrature method. Consequently, the singular integral equation (91) takes the following functional form

$$\sum_{n=0}^{\infty} a_n \left\{ \frac{(1-\nu)\pi}{3-2\nu} U_{n-1}\left(\tilde{x}\right) + h_n\left(\tilde{x}\right) \right\} + \delta\mu Q \sin^{-1}\left(\tilde{x}\right) = 0\,, \quad \left|\tilde{x}\right| < 1\,, \tag{93}$$

with $h_n\left(\tilde{x}\right) = \int_{-1}^{1} T_n\left(\tilde{t}\right)\left(1-\tilde{t}^2\right)^{-1/2} \tilde{N}\left(\tilde{x}-\tilde{t}\right) d\tilde{t}$.

Now, Eq. (93) is solved by truncating the series at $n = N$ and using an appropriate collocation technique with collocation points chosen as the roots of $U_N\left(\tilde{x}\right)$, viz. $\tilde{x}_j = \cos\left(j\pi/\left(N+1\right)\right)$ with $j = 1, 2, ..., N$. In this way, a system of N linear algebraic equations is formed that enables us to evaluate the remaining N coefficients a_n ($n = 1, ..., N$) and, consequently, the desired pressure distribution.

6.2 Separation problem ($c < b$)

Increasing the values of τ (Eq. (51)), the previous solution predicts tensile contact stresses at the vicinity of the edges of the contact area and thus separation is anticipated to occur in this region

Published in *International Journal of Solids and Structures*, 2015, Vol. 63, pp. 226- 239.
doi:10.1016/j.ijsolstr.2015.03.002

(see Figure 1b). In this case, the solution methodology is similar to the previous one except that the length $2c$ ($c<b$) is now unknown and depends upon τ and the microstructural length scale ℓ.

When the separation regime is considered, the contact tractions are not singular at the separation line $x=\pm c$. Accordingly, bearing in mind that the governing singular integral equation has *qualitatively* the same general form with the respective one in the classical theory (with the addition of the regular kernel), we assume the following pressure distribution under the indentor (Zisis et al. 2014)

$$p(\tilde{t})=\sum_{n=0}^{\infty} b_n U_n(\tilde{t})\left(1-\tilde{t}^2\right)^{1/2} \quad , \ |\tilde{t}|\le 1 \tag{94}$$

In this case, the integral equation in (87) becomes

$$\sum_{n=0}^{\infty} b_n \left\{ -\frac{1-\nu}{3-2\nu}\int_{-1}^{1} \frac{U_n(\tilde{t})\left(1-\tilde{t}^2\right)^{1/2}}{(\tilde{x}-\tilde{t})} d\tilde{t} + \int_{-1}^{1} U_n(\tilde{t})\left(1-\tilde{t}^2\right)^{1/2} \tilde{N}(\tilde{x}-\tilde{t})\, d\tilde{t} \right\} + \delta\mu Q \sin^{-1}(\tilde{x}) = 0, \ |\tilde{x}|<1 \tag{95}$$

The first integral in (95), is evaluated as a CPV integral by using the following relation (Erdogan and Gupta, 1972)

$$\int_{-1}^{1} \frac{U_n(\tilde{t})\left(1-\tilde{t}^2\right)^{1/2}}{(\tilde{x}-\tilde{t})} d\tilde{t} = \pi T_{n+1}(\tilde{x}) \quad \text{for} \quad n\ge 0 \ , \ |\tilde{x}|<1 \ . \tag{96}$$

Accordingly, one reaches the following functional equation that can be used in the numerical discretization

$$\sum_{n=0}^{\infty} b_n \left\{ -\frac{(1-\nu)\pi}{3-2\nu} T_{n+1}(\tilde{x}) + w_n(\tilde{x}) \right\} + \delta\,\mu Q \sin^{-1}(\tilde{x}) = 0 \ , \ |\tilde{x}|<1 \tag{97}$$

where $w_n(\tilde{x})=\int_{-1}^{1} U_n(\tilde{t})\left(1-\tilde{t}^2\right)^{1/2} \tilde{N}(\tilde{x}-\tilde{t})\, d\tilde{t}$ is a regular integral which can be evaluated by the standard Gauss–Chebyshev quadrature method. Eq. (97) is solved by truncating the series at $n=N$

Published in *International Journal of Solids and Structures*, 2015, Vol. 63, pp. 226- 239.
doi:10.1016/j.ijsolstr.2015.03.002

and using an appropriate collocation technique with collocation points chosen as the roots of $T_{N+1}(\tilde{x})$, viz. $\tilde{x}_j = \cos\left((2j-1)\pi/(2(N+1))\right)$ with $j = 1, 2, ..., N+1$ which is solved in the least square sense. In this way, a system of $N+1$ linear algebraic equations is formed for the $N+1$ coefficients b_n. It is noted that since the index of the pertinent singular integral equation is: $\kappa = -1$, the complementary condition (54) is not necessary for the computation of the system coefficients but is essential for the evaluation of the unknown contact area $2c$. In general, in such cases where no stress singularity occurs at the ends of the contact area, a consistency condition should be also considered (see e.g. Gakhov, 1966). However, it can be shown that in our case this condition is identically satisfied. Finally, in order to avoid iterations, it is instrumental to assume the contact length c and the ratio ℓ/c as given values for computing the required value of the dimensionless parameter τ in (51) and accordingly the pressure, for a given Poisson's ratio and indented load P.

7. Results and discussion

We now proceed to the discussion of the numerical results. In classical thermoelasticity, the single dimensionless parameter τ, which is defined in (51) and depends upon ν, characterizes completely the response of the system and the type of contact (Comninou et al., 1981). On the other hand, in the couple-stress elasticity formulation the Poisson's ratio has an explicit effect in both the mechanical and the thermal responses of the medium and, thus, should be treated independently (an analogous situation was encountered in Muki and Sternberg, 1965; and Zisis et al., 2014). For this reason, in the present study, a more appropriate definition of such a dimensionless parameter would be the following,

$$\tau^* = \frac{\mu\alpha bQ}{kP} = \frac{1-\nu}{1+\nu}\tau \ . \tag{98}$$

The limit values of τ (τ^*_{crit} or τ_{crit}) defining the transition from perfect contact to separation for the microstructured solid are also dictated by the dimensionless parameter ℓ/b, as illustrated in Figure 2. For clarity and for direct comparison with the classical solution of Comninou et al., 1981, results are reported here for both τ^*_{crit} and τ_{crit}.

Published in *International Journal of Solids and Structures*, 2015, Vol. 63, pp. 226- 239.
doi:10.1016/j.ijsolstr.2015.03.002

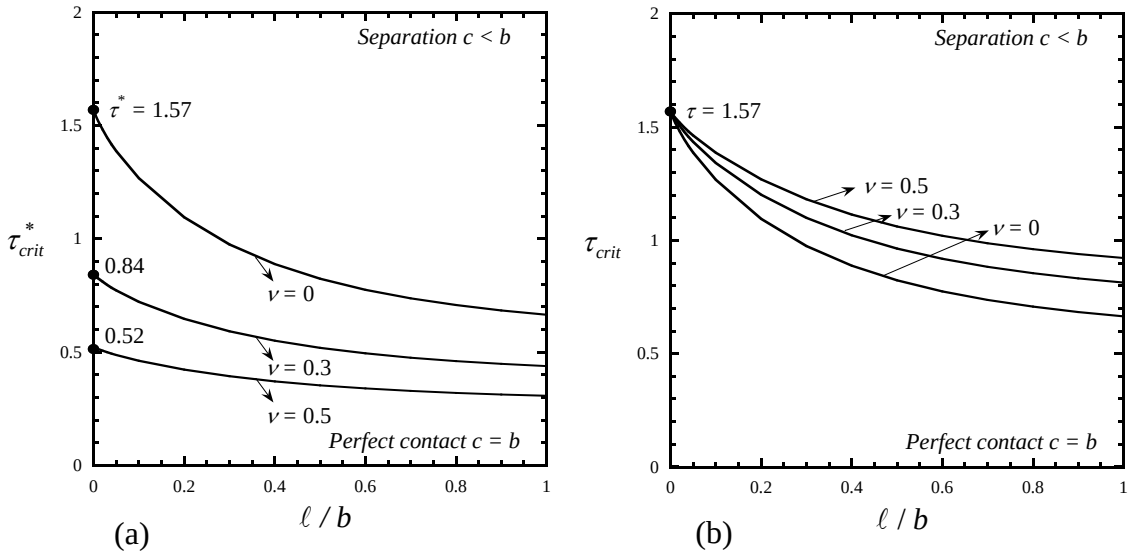

Figure 2: The effect of the microstructural length ℓ/b upon the critical values of the dimensionless parameters τ^*_{crit} and τ_{crit}. The critical values of (a) τ^*_{crit} or (b) τ_{crit} that define the type of contact depend strongly upon ℓ/b. The region below each curve suggests perfect contact while the region above suggests separation.

Figure 2 depicts the dependence upon the ratio ℓ/b of the critical values of the dimensionless parameters τ^*_{crit} and τ_{crit} at which separation succeeds perfect contact. In Figure 2b, at the limit $\ell/b=0$ (classical thermoelasticity), all curves converge to the value $\tau_{crit}\approx 1.57$ (Comninou et al., 1981) independently of the Poisson's ratio. As it was shown by Comninou et al., 1981, for $\tau_{crit}>1.57$ (or $\tau^*_{crit}>\{1.57;0.84;0.52\}$ for $\nu=\{0;\,0.3;\,0.5\}$, respectively) separation occurs at the punch corners leaving a reduced contact area. On the other hand, in the case of couple–stress thermoelasticity this result is affected by the internal length scale. It is observed that as ℓ/b increases, the value of the parameter τ^*_{crit} decreases monotonically attaining a constant value depending upon the Poisson's ratio ν. This implies that in a microstructured material separation will occur for smaller values of the ratio Q/P. For example, and for the range of calculations that are carried out in the present work, at $\ell/b=1$ and $\nu=0$ the parameter τ^*_{crit} decreases by about 50% suggesting that separation

Published in *International Journal of Solids and Structures*, 2015, Vol. 63, pp. 226- 239.
doi:10.1016/j.ijsolstr.2015.03.002

characteristics will be attained at essentially half the Q/P ratio that corresponds to classical thermoelasticity.

7.1 Perfect contact ($c = b$)

Within the perfect contact regime a square root singularity in the pressure distribution is observed at the sharp edges of the punch as in the case of classical thermoelasticity (Figure 3). In the limit $\ell/b = 0$, the present results reduce to the corresponding ones attained for the classical thermoelasticity (Comninou et al., 1981), while in the limit $\tau^* = 0$ reduce to those attained by Muki and Sternberg (1965) and Zisis et al. (2014). We should note that, excluding the thermal effects, as ℓ / b increases from zero, the results regarding the pressure below the indenter depart from those predicted by classical elasticity. In fact, it is has been shown by Muki and Sternberg (1965) and Zisis et al. (2014) that at small values of the ratio ℓ / b the couple-stress effects are more pronounced leading to an increased deviation from the classical elasticity solution. The boundary layer effect near the corners of the punch is more apparent for $x / b = 0.99$ and $x / b \to 1^-$, where the pressure below the indenter with increasing ℓ / b follows an initial steep descent below the classical pressure-ratio of unity, then rises to a maximum above unity and finally steadily approaches the asymptotic value of unity as $\ell/b \to \infty$. Furthermore, it has been shown that deviation from the classical elasticity solution, even though less pronounced, is not only attained near the punch corners ($x / b = 0.99$) but also close to the center of the punch ($x / b = 0$) for small ratios of ℓ / b.

It is observed that, for fixed ℓ/b, as τ^* increases, departing from $\tau^* = 0$ (no thermal effects), the pressure below the indentor increases at the center of the contact ($x = 0$). A stiffer response is attained for increasing Poisson's ratio (Figure 3). Moreover, as it is illustrated in Figure 3, for a microstructured material with $\ell/b = 0.2$, the transition between the two types of contact is attained at $\tau^* = 1.095$ for $\nu = 0$, and $\tau^* = 0.423$ for $\nu = 0.5$ (dashed lines in Figure 3). In these cases, the pressure at the corners of the indentor is bounded and equal to zero.

Published in *International Journal of Solids and Structures*, 2015, Vol. 63, pp. 226- 239.
doi:10.1016/j.ijsolstr.2015.03.002

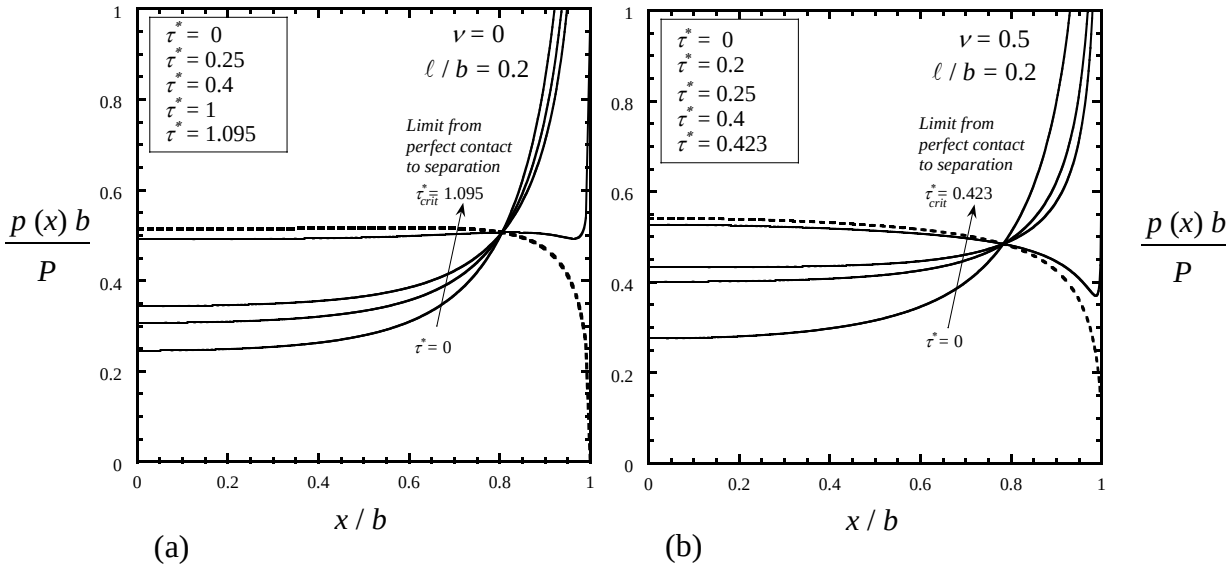

Figure 3: Pressure distributions for selected values of τ^* at fixed ℓ/b for Poisson's ratio (a) $\nu = 0$ and (b) $\nu = 0.5$. Only half of the indentor ($x \geq 0$) is presented due to symmetry. Results for the limit value of τ^* at the corresponding ℓ/b and ν are also shown (- - -).

The influence of couple-stresses upon the pressure distribution is brought out more clearly in Figure 4, where the ratio of the modified to the classical pressure $p(x)/p_{cl}(x)$ is plotted as a function of x/b for various values of ℓ/b, τ^* and ν. It is observed that for increasing τ^*, the pressure below the indentor increases and is affected by the magnitude of the normalized characteristic length ℓ/b and the Poisson's ratio ν. An evident deviation from the classical pressure distribution is found, at small values of ℓ/b, in a relative narrow band near the corners of the punch, revealing thus a boundary layer effect.

Published in *International Journal of Solids and Structures*, 2015, Vol. 63, pp. 226- 239.
doi:10.1016/j.ijsolstr.2015.03.002

Published in *International Journal of Solids and Structures*, 2015, Vol. 63, pp. 226- 239.
doi:10.1016/j.ijsolstr.2015.03.002

These results may also be seen in conjunction with Figure 5. When thermal effects are excluded (τ^*=0), the curves depart from and then approach the classical elasticity results as ℓ/b increases from zero. Indeed, the limiting values of $p_0 \equiv p(0)$ at $\ell/b = 0$ and $\ell/b \to \infty$ coincide (see Muki and Sternberg, 1967 and Zisis et al., 2014). On the other hand when $\tau^* > 0$, the behavior is strongly influenced by the deformation induced by the thermal effects. The dashed line suggests the limiting values of the ratio ℓ/b at fixed τ^* further from which the type of contact changes from perfect to separation. Results are shown only for the case of perfect contact throughout the flat punch. The classical thermoelasticity solution is represented by the single points at $\ell/b = 0$. For all the cases, as ℓ/b increases from zero, the pressure below the indentor departs from that predicted by the classical thermoelasticity, initially decreases and then increases again attaining a constant value (greater than the classical thermoelasticity solution) as $\ell/b \to \infty$ that depends upon τ^*. For example, when $\nu = 0$ and $\tau^* = 0.75$ the pressure below the indentor at $x = 0$ reduces to a minimum value attained at $\ell/b \approx 0.2$ and then rapidly increases with increasing ℓ/b up to $p_0 b/P \approx 0.55$. Further increase of ℓ/b (for $\tau^* = 0.75$) suggests that the contact characteristics will change and separation near the corners of the punch will be attained. Similar results can be observed in the incompressible limit $\nu = 0.5$.

Finally, we note that since the singular fields for sharp edge contacts and for cracked bodies suggest similarities (Giannakopoulos et al, 1998), it is of interest to present an equivalent to the Mode I stress intensity factor for a double edge cracked infinite plate (containing two semi-infinite cracks whose tips are separated by a distance of $2b$). The equivalent stress intensity factor in couple-stress elasticity (given here for the right edge) is defined as

$$K_I = \lim_{x \to b^-} \left(p(x) \sqrt{2\pi (b - x)} \right), \tag{99}$$

whereas in the classical elasticity case, the respective stress intensity factor is: $K_{I,class} = P(\pi b)^{-1/2}$ corresponding to a pressure distribution $p_{cl}(x) = P\pi^{-1}\left(b^2 - x^2\right)^{-1/2}$.

Published in *International Journal of Solids and Structures*, 2015, Vol. 63, pp. 226- 239.
doi:10.1016/j.ijsolstr.2015.03.002

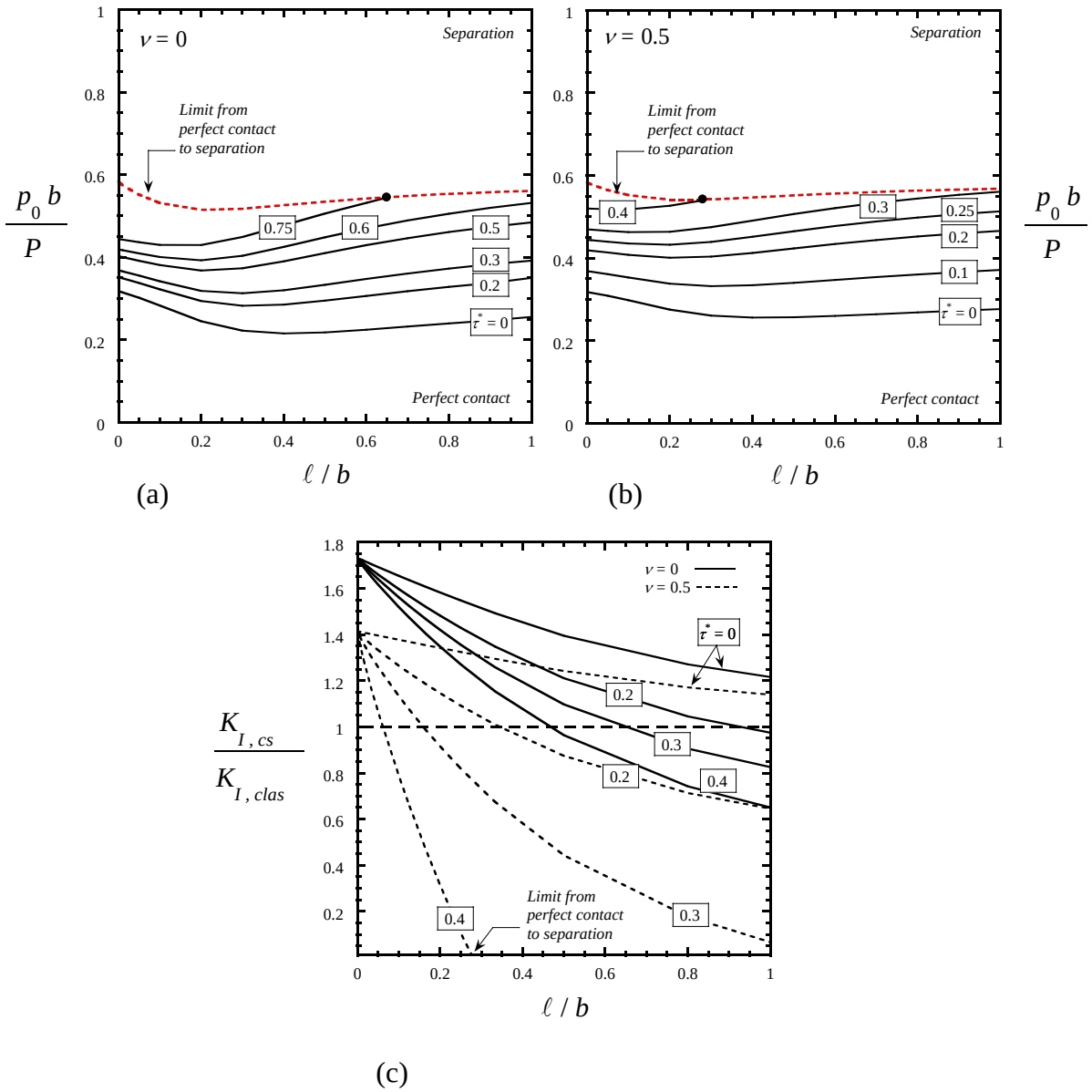

Figure 5: Normalized pressure $p_0 b/P$ as a function of the normalized micromechanical length ℓ/b for selected values of τ^* for Poisson's ratios (a) $\nu = 0$ and (b) $\nu = 0.5$. The values of p_0 at the limit between perfect contact and separation are also shown. (c) Normalized stress intensity factor for the analogous to the flat punch contact problem infinite plate with a double edged crack as a function of ℓ/b and selected values of τ^* and Poisson's ratios.

Published in *International Journal of Solids and Structures*, 2015, Vol. 63, pp. 226- 239.
doi:10.1016/j.ijsolstr.2015.03.002

The variation of the ratio $K_{I,cs}/K_{I,clas}$ (for the same values of the parameter τ^*) with respect to ℓ/b is illustrated in Figure 5(c). It is observed that the ratio exhibits a finite jump discontinuity at $\ell/b \to 0$, indeed, $K_{I,cs}/K_{I,clas}$ rises abruptly as ℓ/b departs from zero and then declines monotonically with increasing values of ℓ/b. This discontinuous behavior appears to be typical of the severe boundary-layer effects predicted by the couple-stress theory in singular stress-concentration problems (Muki and Sternberg, 1965; Zisis et al., 2014; Gourgiotis and Piccolroaz, 2014). Furthermore, it is noted that as τ^* increases the ratio $K_{I,cs}/K_{I,clas}$ falls below unity. In particular, when τ^* grows beyond a critical value $\tau^* > \tau^*_{crit}$ the ratio $K_{I,cs}/K_{I,clas}$ becomes zero for certain values of ℓ/b (e.g. dashed curve - $\nu = 0.5$ and $\tau^* = 0.4$). This is due to the fact that the separation in couple-stress elasticity occurs in lower values of τ^*_{crit} than on the classical elasticity case (see Figure 2).

7.2 Separation ($c < b$)

Further increase of τ^* and depending upon the characteristic material length ℓ and Poisson's ratio ν, separation will occur at the edges of the punch leaving a region of perfect contact $2c$ with $c < b$. Figure 6 presents pressure distributions below the punch for different values of τ^* at fixed ℓ/c and pressure distributions for different values of ℓ/c at fixed τ^*. The effect of Poisson's ratio is also shown. It is concluded that as τ^* increases, the contact width reduces, increasing the pressure below the indentor. The response is similar for increasing microstructural length ℓ/c. As intuitively expected, the stiffness of the response increases with increasing Poisson's ratio.

Finally, results regarding the contact width and the average pressure $p_{av} = P/2c$ are summarized in Figures 7a and 7b and their dependence upon the microstructural length ℓ for different values of τ^* and different Poisson's ratios ν is explored. It is observed that for increasing ℓ/c, increasing ν and increasing τ^* the measured contact width decreases, while the average pressure increases suggesting a stiffer material response. It can be seen that at the two classical ($\ell/c = 0$) thermoelasticity limits $\tau^*_{crit} = 1.57$ and $\tau^*_{crit} = 0.524$ for $\nu = 0$ and $\nu = 0.5$ respectively, no separation is observed (i.e. $c/b = 1$) as expected but immediately for increasing values of ℓ/c the contact changes from perfect to separation. For smaller values of τ^* the contact is perfect throughout

Published in *International Journal of Solids and Structures*, 2015, Vol. 63, pp. 226- 239.
doi:10.1016/j.ijsolstr.2015.03.002

the flat punch up to a certain value of the ratio ℓ/c. Beyond this limit the contact type changes to separation at the edges of the indenter. For example, as it is shown in Figure 7a, for $(\tau^*,\nu)=(1,0)$ or $(\tau^*,\nu)=(0.4,0.5)$ perfect contact is attained up to $\ell/c<0.3$, however, for further increase of ℓ/c separation will take place at the edges of the indenter.

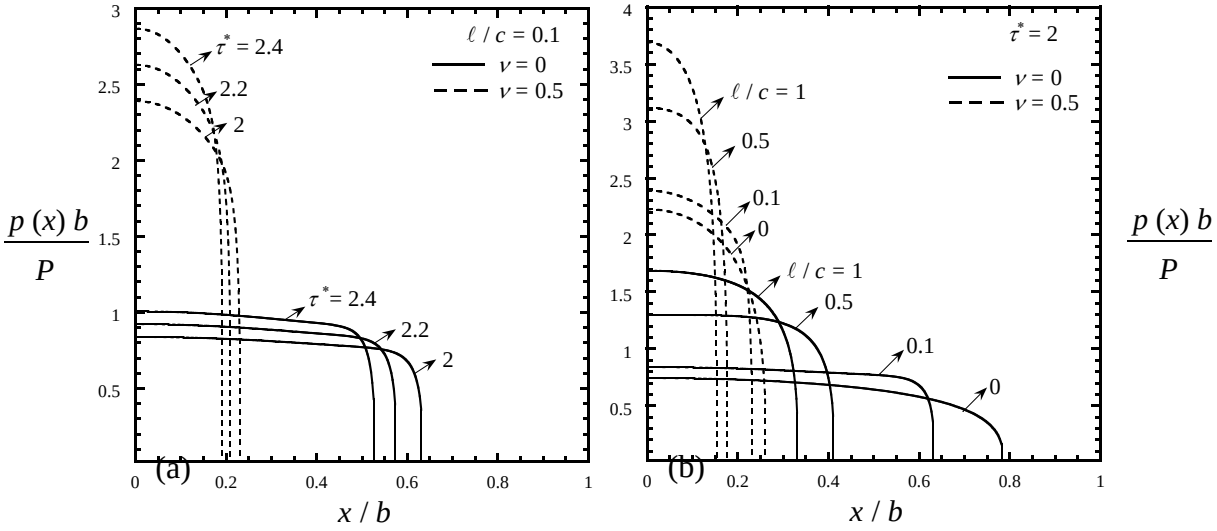

Figure 6: Pressure distributions for (a) selected values of τ^* at fixed ℓ/c and (b) selected values of ℓ/c at fixed τ^*. Only half of the domain is presented due to symmetry. Results are shown for Poisson's ratios $\nu=0$ and $\nu=0.5$.

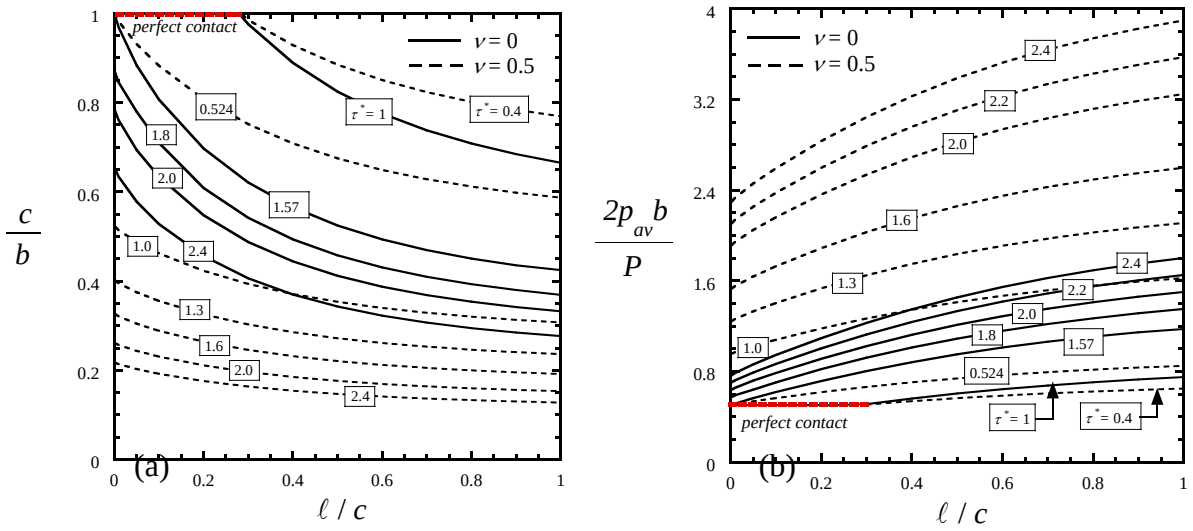

Figure 7: (a) The normalized contact width c/b and (b) the normalized average pressure $2p_{av}b/P$ exerted at the indentor. Both are shown as functions of the micromechanical length ℓ/c for selected values of τ^*. Results are shown for Poisson's ratio $\nu=0$ and $\nu=0.5$.

Published in *International Journal of Solids and Structures*, 2015, Vol. 63, pp. 226- 239.
doi:10.1016/j.ijsolstr.2015.03.002

8. Conclusions

In the present study, we derived general solutions for a basic two–dimensional plane strain contact problem within the framework of the generalized continuum theory of couple–stress thermoelasticity. The problem of the indentation of a deformable half–plane by a hot flat punch has been investigated, solving the singular integral equations resulted from a treatment of the mixed boundary value problems via integral transforms and generalized functions.

The attained solution describes a mechanical response strongly affected by the characteristic material length, exhibiting significant departure from the predictions of classical thermoelasticity. Indeed, when the material microstructure is taken into account ($\ell \neq 0$), the limits in terms of heat flux (assuming fixed applied load and material properties) at which the type of contact transits from perfect to separation vary significantly compared to the classical thermoelasticity results (Comninou et al., 1981). Moreover, as the characteristic material length ℓ increases, with respect to the contact width, a stiffer material response is attained.

In light of the above, contact phenomena in microstructured materials cannot be adequately described through classical contact mechanics.

Appendix

Here, we show that the last terms on the RHS of Eqs. (72) and (73) respectively, are equal, i.e.

$$-\frac{1}{2\pi}\int_{-\infty}^{\infty}\left(\frac{(1-2\nu)\beta}{2\mu}\frac{i}{\xi}\frac{d\hat{\theta}}{dy}\right)e^{-ix\xi}d\xi=\delta\int_0^x q(t)\,dt\ . \tag{A1}$$

where δ is the distortivity defined as $\delta=(1-2\nu)\beta/2\mu k=(1+\nu)\alpha/k$.

To this end, we define the function

$$F(x)=-\frac{1}{2\pi}\int_{-\infty}^{\infty}\frac{i}{\xi}\frac{d\hat{\theta}(\xi,0)}{dy}e^{-ix\xi}d\xi\ . \tag{A2}$$

Differentiating with respect to x and recalling that $\hat{q}(\xi)=-k\,d\hat{\theta}(\xi,0)/dy$, yields

Published in *International Journal of Solids and Structures*, 2015, Vol. 63, pp. 226- 239.
doi:10.1016/j.ijsolstr.2015.03.002

$$\frac{dF(x)}{dx} = -\frac{1}{2\pi}\int_{-\infty}^{\infty} \frac{d\hat{\theta}(\xi,0)}{dy} e^{-ix\xi} d\xi = \frac{1}{2\pi k}\int_{-\infty}^{\infty} \hat{q}(\xi) e^{-ix\xi} d\xi = \frac{q(x)}{k} \ , \tag{A3}$$

and, accordingly

$$F(x) = \frac{1}{k}\int_{-c}^{x} q(t)\,dt + d_0 , \tag{A4}$$

where d_0 is an arbitrary constant. Due to the symmetry of the problem, the heat flux $q(x)$ is an even function for $|x| < c$ and, thus, $F(x)$ is odd with $F(c) = -F(-c)$. Then, using (A4) and the complementary condition in $(48)_1$, we obtain

$$F(c) = \frac{1}{k}\int_{-c}^{c} q(t)\,dt + d_0 = \frac{Q}{k} + d_0 \qquad \text{and} \qquad F(-c) = d_0 \tag{A5}$$

and, consequently, $d_0 = -Q/2k$.

In view of the above, Eq. (A4) can be finally written as

$$F(x) = \frac{1}{k}\int_{-c}^{x} q(t)\,dt - \frac{Q}{2k} = \frac{1}{k}\int_{-c}^{0} q(t)\,dt + \frac{1}{k}\int_{0}^{x} q(t)\,dt - \frac{Q}{2k} = \frac{1}{k}\int_{0}^{x} q(t)\,dt \ , \tag{A6}$$

which readily shows that (A1) holds.

Acknowledgements

Support from the European Union FP7 project "Mechanics of refractory materials at high–temperature for advanced industrial technologies" under contract number PIAPP–GA–2013–609758 is gratefully acknowledged.

Published in *International Journal of Solids and Structures*, 2015, Vol. 63, pp. 226- 239.
doi:10.1016/j.ijsolstr.2015.03.002

References

Abramowitz, M., Stegun, I.A., 1972. Handbook of Mathematical Functions. Dover, New York.

Anderson, W., Lakes, R., 1994. Size effects due to Cosserat elasticity and surface damage in closed-cell polymethacrylimide foam. Journal of Materials Science 29, 6413-6419.

Askar, A., Cakmak, A., 1968. A structural model of a micropolar continuum. Int. J. Eng. Sci. 6, 583-589.

Bacca, M., Bigoni, D., Dal Corso, F., Veber, D. 2013a. Mindlin second-gradient elastic properties from dilute two-phase Cauchy-elastic composites Part I: Closed form expression for the effective higher-order constitutive tensor. Int. J. Solids Struct. 50, 4010-4019.

Bacca, M., Bigoni, D., Dal Corso, F., Veber, D. 2013b. Mindlin second-gradient elastic properties from dilute two-phase Cauchy-elastic composites Part II: Higher-order constitutive properties and application cases. Int. J. Solids Struct. 50, 4020-4029.

Bacigalupo, A., 2014. Second-order homogenization of periodic materials based on asymptotic approximation of the strain energy: formulation and validity limits. Meccanica 49 (6), 1407-1425.

Bacigalupo, A., Gambarotta, L., 2013. A multi-scale strain-localization analysis of a layered strip with debonding interfaces. Int. J. Solids Struct. 50 (13), 2061-2077.

Barber., J.R., 1971. The effect of thermal distortion on constriction resistance. Int. J. Heat Mass Tran. 14 751–766.

Barber., J.R., 1973. Indentation of the semi–infinite elastic solid by a hot sphere. Int. J. Mech. Sci., 15, 813–819.

Barber., J.R., 1978. Contact problems involving a cooled punch. J. Elast. 8, 404–423.

Begley, M.R., Hutchinson, J.W., 1998. The mechanics of size–dependent indentation. J. Mech. Phys. Solids 46, 2049–2068.

Beveridge, A.J., Wheel, M.A., Nash, D.H., 2013. The micropolar elastic behaviour of model macroscopically heterogeneous materials. Int. J. Solids Struct. 50, 246–255.

Bigoni, D., Drugan, W.J., 2007. Analytical Derivation of Cosserat Moduli via Homogenization of Heterogeneous Elastic Materials. ASME J. Appl. Mech. 74, 741–753.

Bower, A.F., 2009. Applied mechanics of solids. CRC Press, Boca Raton, FL.

Chen, X., Hutchinson, J.W., Evans, A.G., 2004. Simulation of the high temperature impression of thermal barrier coatings with columnar microstructure. Acta Mater. 52, 565–571.

Chen, J., Huang, Y., Ortiz, M., 1998. Fracture analysis of cellular materials: A strain gradient model. J. Mech. Phys. Solids 46, 789-828.

Clausing, A.M., 1966. Heat transfer at the interface between dissimilar metals–the influence of thermal strain. Int. J. Heat Mass Tran. 9, 791–801

Comninou, M., Dundurs, J., 1979. On the Barber boundary conditions for thermo-elastic contact. ASME J. Appl. Mech. 8, 849–853.

Comninou, M., Barber., J.R., Dundurs, J., 1981. Heat conduction through a flat punch. J. App. Mech. 48, 871–875.

Dal Corso, F., Willis, J.R. 2011. Stability of strain gradient plastic materials. J. Mech. Phys. Solids 59, 1251-1267.

Danas, K., Deshpande, V.S., Fleck, N.A., 2012. Size effects in the conical indentation of an elasto–plastic solid. J. Mech. Phys. Solids 60, 1605–1625.

Erdogan, F., 1978. Mixed boundary–value problems in mechanics, in: Nemat–Nasser, S. (Ed.), Mechanics today. Pergamon Press, New York, pp. 1–86.

Erdogan, F., Gupta, G.D., 1972. On the numerical solution of singular integral equations. Q. Appl. Math. 29, 525–534.

Fleck, N.A., Zisis, Th., 2010. The erosion of EB–PVD thermal barrier coatings: The competition between mechanisms. Wear 268, 1214–1224.

Gakhov, F.D., 1966. Boundary Value Problems. Pergamon Press and Addison–Wesley, Oxford.

Georgiadis, H. G., 2003. The mode-III crack problem in microstructured solids governed by dipolar gradient elasticity: Static and dynamic analysis, ASME J. Appl. Mech. 70, 517-530.

Giannakopoulos, A.E., Lindley, T.C., Suresh, S. 1998. Aspects of equivalence between contact mechanics and fracture mechanics: theoretical connections and a life-prediction methodology for fretting-fatigue. Acta Mat., 46 (9), 2955-2968.

Gourgiotis, P.A., Piccolroaz, A. 2014. Steady-state propagation of a Mode II crack in couple stress elasticity. Int. J. Fract. 188, 119-145.

Green, A.E., Adkins, E., 1960. Large Elastic Deformations. Oxford.

Han, C.-S., Nikolov, S., 2007. Indentation size effects in polymers and related rotation gradients. J. Mater. Res. 22, 1662-1672.

Hills, D.A., Nowell, D., Sackfield, A., 1993. Mechanics of Elastic Contact. Butterworth–Heinemann, Oxford.

Johnson, K., 1985. Contact Mechanics. Cambridge University Press, Cambridge, UK.

Koiter, W., 1964. Couple stresses in the theory of elasticity. Parts I and II. Nederl. Akad. Wetensch. Proc. Ser. B. 67, 17–29.

Lakes, R., 1986. Experimental microelasticity of two porous solids. Int. J. Solids Struct. 22, 55-63.

Lakes, R., 1995. Experimental methods for study of cosserat elastic solids and other generalized elastic continua. Continuum models for materials with microstructure, 1-25.

Lakes, R.S., Gorman, D., Bonfield, W., 1985. Holographic screening method for microelastic solids. J. Mater. Sci. 20, 2882–2888.

Larsson, P.L., Giannakopoulos, A.E., Söderlund, E., Rowcliffe, D.J., Vestergaard, R., 1996. Analysis of Berkovich indentation. Int. J. Solids Struct. 33, 221-248.

Maugin, G.A., 2010. Generalized continuum mechanics: what do we mean by that? In: Maugin, G.A., Metrikine, A.V. (Eds.), Mechanics of Generalized Continua. Springer, New York, pp. 3–13.

Maranganti, R., Sharma, P., 2007. Length scales at which classical elasticity breaks down for various materials. Phys. Rev. Lett. 98, 195504.

Mindlin, R.D., 1963. Influence of couple–stresses on stress concentrations. Exp. Mech. 3, 1–7.

Mindlin, R.D., Tiersten, H.F., 1962. Effects of couple–stresses in linear elasticity. Arch. Ration. Mech. Anal. 11, 415–448.

Muki, R., Sternberg, E., 1965. The influence of couple–stresses on singular stress concentrations in elastic solids. Z. Angew. Math. Phys. (ZAMP) 16, 611–648.

Naghdi, P.M., 1965. A Static-geometric analogue in the theory of couple-stresses. Nederl. Akad. Wetensch. Proc. Ser. B. 68, 29–32.

Nikolov, S., Han, C.S., Raabe, D., 2007. On the origin of size effects in smal-strain elasticity of solid polymers. Int. J. Solids Struct. 44, 1582-1592.

Nix, W.D., Gao, H., 1998. Indentation size effects in crystalline materials: A law for strain gradient plasticity. J. Mech. Phys. Solids 46, 411–425.

Nowacki, W., 1966. Couple stresses in the theory of thermoelasticity I. Bulletin de L' Academie Polonaise des Sciences, Serie des sciences techniques Volume XIV, No. 2.

Nowacki, W. 1986. Theory of Asymmetric Elasticity. Oxford, Pergamon Press.

Onck, P., Andrews, E., Gibson, L., 2001. Size effects in ductile cellular solids. Part i: Modeling. Int. J. Mech. Sci. 43, 681-699.

Poole, W.J., Ashby, M.F., Fleck, N.A., 1996. Micro–hardness of annealed and work–hardened copper polycrystals. Scripta Mater. 34, 559–564.

Published in *International Journal of Solids and Structures*, 2015, Vol. 63, pp. 226- 239.
doi:10.1016/j.ijsolstr.2015.03.002

Shu, J.Y., Fleck, N.A., 1998. The prediction of a size effect in microindentation. Int. J. Solids Struct. 35, 1363–1383.

Smyshlyaev, V.P., Fleck, N.A., 1995. Bounds and estimates for the overall plastic behavior of composites with strain gradient effects. Phil. Trans. R. Soc. A. 451, 795-810.

Stupkiewicz, S., 2007. Micromechanics of contact and interface layers. Lecture Notes in Applied and Computational Mechanics, vol. 30. Springer, Berlin.

Reid, A.C.E., Gooding, R.G., 1992. Inclusion problem in a two–dimensional nonlocal elastic solid. Phys. Rev. B 46, 6045–6049.

Roos, B.W., 1969. Analytic Functions and Distributions in Physics and Engineering. Wiley, New York.

Zhang, X., Sharma, P., 2005a. Inclusions and inhomogeneities in strain gradient elasticity with couple stresses and related problems. Int. J. Solids Struct. 42, 3833–3851.

Zhang, X., Sharma, P., 2005b. Size dependency of strain in arbitrary shaped anisotropic embedded quantum dots due to nonlocal dispersive effects. Phys. Rev. B 72, 195345–1–195345–16.

Zisis, Th., Gourgiotis, P.A., Baxevanakis, K.P. and Georgiadis, H.G., 2014. Some basic contact problems in couple stress elasticity, Int. J. Solids Struct. 51, 2084–2095.

Zisis, Th., Fleck, N.A., 2010. The elastic–plastic indentation response of a columnar thermal barrier coating. Wear 268, 443–454.

Wei, Y., Hutchinson, J.W., 2003. Hardness trends in micron scale indentation. J. Mech. Phys. Solids 51, 2037–2056.